Transverse Load Versus Mechanical Characteristics and Inter-Strand Resistances in the Cable of the "Option 2" Specification for ITER TF Conductor

Dong Keun Oh, Sangjun Oh, Hyoung Chan Kim, Heekyung Choi, Chulhee Lee, Wonwoo Park, and Keeman Kim

***Abstract*—A revised specification of ITER TF conductor was proposed as "Option2" for the baseline design. The cabling pitches of early stages and the void fraction were adjusted in the consequence of previous R&D programs to improve the degradation of performance against cyclic current loadings in the magnetic field. To obtain the characteristics of the developed design, which are related to the effect of the electromagnetic load, the mechanical parameters and the contact resistances between components of cable were investigated employing a specially developed device of cryogenic press in the transverse direction for a short sample of the conductor cable. Through the measurements, the mechanical characteristics against the cyclic loads were discussed, as well as the effect on inter-strand resistances, according to the cable design.**

***Index Terms*—CICC, contact resistance, cryogenic press, ITER, mechanical property, Nb_3Sn, TF conductor.**

I. Introduction

THE 'Option2' was specified, as a recent update of the design of ITER TF conductor, to overcome a known problem of the previous baseline, the performance degradation with respect to cyclic loadings [1]. Keeping the existing design concept as much as possible, the "Option2" specifies only slightly modified dimensions of components with the same cabling scheme as shown in the Table I so that it present the major changes in the void fraction and the twist pitches based on the previous R&D result [2] to improve the performance of the previous baseline which is now called as "Option1". Such an attempt has been successfully verified through the conductor performance tests which have been carried out with "Option2" short samples fabricated by several participants for the prequalification process as a part of the TF conductor procurement plan.

In the "Option2", one of the key aspects to the design is longer twist pitches which are employed according to the previous result of TFPRO2 (OST2 with internal-tin strands of Oxford Inc.) conductor of EU-DA with long twist pitches, which showed significant improvement in T_{cs} value among the samples tested in the R&D phase [3]. Furthermore, a theoretical evaluation also supported the idea of long twist pitch based on the elastic model for the deformation of strands and cable with respect to the cabling pitches [4]. On the other hand, the jacket thickness is increased to reduce the void fraction to ~29% with an aim to enhance the mechanical strength of conductor at the same time. To decrease the void fraction, a wider central channel is also introduced moderating the pressure drop caused by the reduction of annular space at the same time.

TABLE I
DIMENSIONAL PARAMETERS OF ITER TF OPTION2 CONDUCTOR

Cabling Scheme	6 sub-cables (petals) + central channel Sub-cable = (2S/C + 1Cu) × 3 × 5 ×5 + 3 × 4 Cu
Twist Pitch (mm)	(80/140/190/300+80/140)/420
Strand Dimension	OD=0.820~0.821 mm, Cr plating=1.8 μm
Jacket (316LN-IG-HT) after Fabrication	O.D = 43.7 mm (±0.1 mm) I.D = 39.9 mm (±0.1 mm) Thickness = 2.0 mm (±0.1 mm)
Central Channel (316L or 304L)	OD = 10 mm (±0.1 mm), Thickness = 1.0 mm (±0.05 mm), Strip Width = 6 mm, Twist Pitch = 9 mm,
Void Fraction	~29 %

As a matter of course, the robust performance of "Option2" conductors is closely related to the actual environment for micro-mechanical displacements of each strand in the cable against to the load, which is strongly affected by cabling parameters i.e. the void fraction and the twist pitches of each stage, being reflected on the mechanical properties of the cable itself [5]. Thus, to understand the robustness against the degradation, more attention should be paid to the mechanical response of the cable with respect to repeated transverse loads in cryogenic condition.

Cryogenic press has been employed to investigate the mechanical parameters and the AC-loss of cable as well as the contact resistances between strands of full size superconducting cables under the transverse mechanical load which simulates Lorentz force on the conductor, at the University of Twente [5]–[7]. A similar device has been built as a research activity in NFRI since 2005 to study the effect of transverse load on the CIC conductor with respect to the void fraction. The contact resistance measurement was also implemented, which is one of the important properties related to the cabling patterns and the void fraction. Those characteristics under the transversal load will primarily depend on the void fraction so that the built device is called as VOFEX (VOid Fraction EXperiment).

Manuscript received October 20, 2009. First published April 05, 2010; current version published May 28, 2010. This work was supported by the Korean Ministry of Science and Technology of Republic of Korea under the Contract of ITER Korea Project (2009-0081593).

The authors are with the National Fusion Research Center, Daejeon, Republic of Korea (e-mail: kkeeman@nfri.re.kr).

Digital Object Identifier 10.1109/TASC.2010.2043835

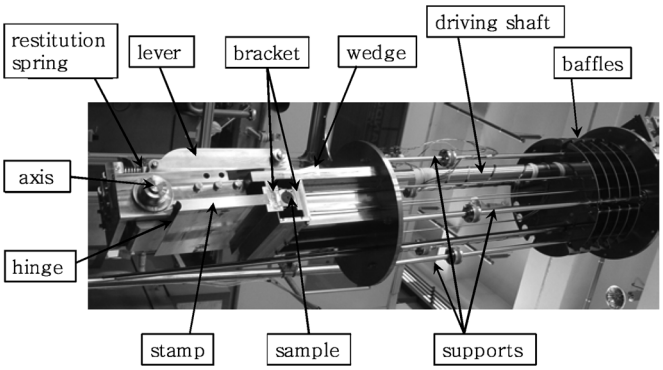

Fig. 1. The picture of VOFEX cryopress, which was taken during the campaign for "Option2" being ready for the cool-down (the picture is rotated in 90 °).

After a successful test run of VOFEX device, we planned a test with a short piece of the "Option2" conductor [8] to understand the mechanical properties which were expected to have a close relation to the performance degradation with respect to the repetitive transverse loads.

II. Experiment

However, the mechanical part of VOFEX device is capable of the transverse load above 20 MPa, care had to be taken for the maximum load to be limited according to the condition for the ITER TF magnet whose maximum Lorentz force is estimated to be 802.4 kN/m ($\mathrm{I} = 68$ kA and $\mathrm{B} = 11.81$ Tesla) which corresponds to 16 MPa on the cryogenic press in VOFEX device.

Pressure were detected by 6 strain gauges attached in vertical direction on the sides of the pressure sensing plates laid on the bottom bracket for a square jacket of the sample conductor. A piece of sample was obtained from the fabricated CICC for the prequalification test (TFKO2, Option2, K.A.T. RC49 internal-tin strand) [8]. Four displacement transducers were also applied to monitor the vertical displacement between the upper and the lower piece of the square jacket. A Vishay 5100 scanner was employed to measure the pressure (6 quarter bridges) and the displacement (4 half bridges).

To apply transversal load, the cryogenic press was controlled by an AC servo system in constant speed to increase the pressure up to the limit of 16 MPa in about 1 minute during the ramping up. Then, pressure was released by reverse rotation of the servo motor at the same speed until the servo reached the initial position. The pressure was measured using the average of 6 channels of 5100 scanner for the gauges on the pressure sensor multiplying the conversion factor which was determined in the former calibration procedure. In such a manner, cyclic loads could be repeated automatically for the specified number of loads. Before all automatic cycles, we recorded the displacement and the pressure for a cycle to obtain the mechanical parameters of the cable, and measured contact resistances between the selected strands at the free and the loaded condition respectively.

The 25 channels of current path were made up from one fixed wire and the other 25 wires being selected to measure the contact resistance between the pairs of strand according to each cabling stage in the same petal and also between the petals. For one plus 25 voltage taps of 4-wire sensing, the voltage drop was detected by a nano-voltmeter (Keithley 2182) through a 40 channel Keithely 7011-S scanner to select the corresponding tap on the strand under the current excitation. Into the pair of strands of which one is fixed, 20 A was loaded multiplexing the output of a KEPCO digital power supply from a home-build 28 channel relay bank (OMRON, G4A-1A-E DC12) which was controlled by a digital board designed for the Gespac-64 bus. In this manner, automatic scanning was possible to measure the contact resistance between selected pair of strands employing polarity reversal for the current to eliminate thermal EMF in the signal.

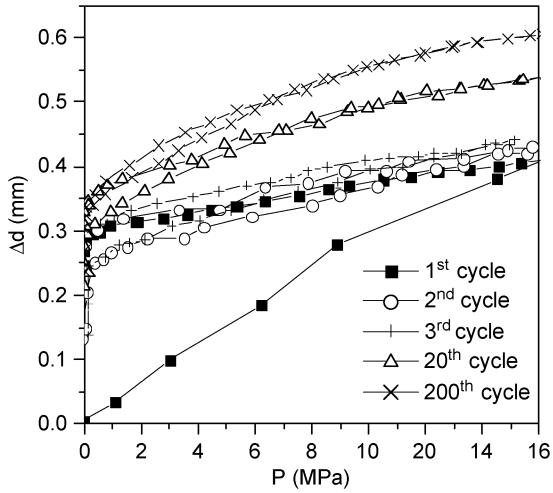

Fig. 2. Displacement versus applied pressure for 5 loading cycles (1st, 2nd, 3rd, 20th, and 200th).

III. Results and Discussion

A. Mechanical Characteristics

During the repeated transverse loads up to 200 cycles, the displacement was observed due to cyclic load of pressure on the conductor jacket. All measurements were carried out in the liquid helium at 4.2 K.

In Fig. 2, datasets at some certain cycles were appeared to show curves of the displacement as a function of the applied pressure. At the virgin condition, the curve showed the initial linear slope up to about 10 MPa. Then, the Young's modulus was evaluated as 2.56 GPa for the initial slope, which has been theoretically estimated as more than ~2 GPa [9].

Right after the initial half of the first cycle, a deformation was observed, which corresponds to the plastic compression as a result of repetitive loadings. With such a deformation, the area of hysteresis loop was decreased significantly after 1st cycle, which means mechanical heat losses will be fairly reduced after the initial loading. The mechanical heat loss could be calculated using

$$\boldsymbol{Q_{Mech}} = \frac{1}{\boldsymbol{L}} \oint \boldsymbol{F} \cdot \boldsymbol{dy} \tag{1}$$

The initial heat loss was evaluated as 103 mJ/m · cycle. Then, the loss was appeared as 22 mJ/m · cycle at 3rd cycle and was saturated into ~ 8 mJ/m · cycle after 20th.

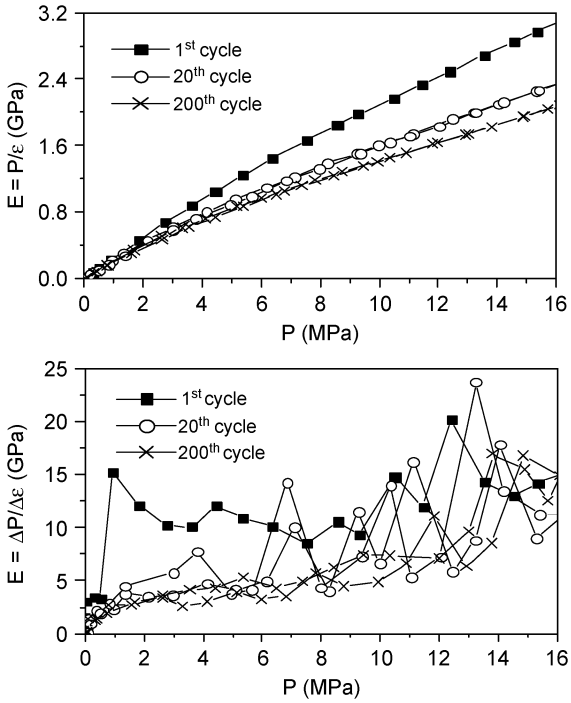

Fig. 3. Pressure dependence of overall Young's modulus (upper) and dynamic modulus (lower).

From the datasets in Fig. 2, the overall Young's modulus and dynamic elastic modulus could be obtained as Fig. 3 through simple formulae in elsewhere [10], [11]. According to the progress of cyclic loads, the overall modulus was decreased due to plastic deformation. The dynamic modulus, which represents the stiffness of cable at certain level of pressure, was 1 $\sim$ 20 GPa at 200 cycle.

B. Contact Resistance Between Strands

As well as the surface condition of Cr plating [4], local tightness on the contact areas can play an important role to determine the contact resistances. The contact resistances itself are not only one of the most important factors for the AC loss of coupling loop of strands [10], [11], which contribute to the total loss of cable as the largest part in most cases, but also can reflect the characteristic of cable design which determines the distribution of crossing points of mechanical contacts between strands or sub-cables. In particular, continuous transverse loads may cause the change of those properties of each sub-stage in different ways so that measuring the contact resistance stage-by-stage can help us monitor the effect of the microscopic deformations in depth, even though they are qualitative information.

Classified into groups with respect to the cabling stage (see Fig. 4), 25 resistance values were measured between the fixed one (1) and strands in the same triplet (2 & 3C), and between the 2nd triplets (4, 5 & 6C), 3rd stage sub-cables (7, 8C, 10, 11 & 24) and 4th stage ones (12, 13C, 14, 15, 16 & 25 which were sampled from different 3rd stage sub-cables, and 17C & 26C from the Cu core of 4th stage). The inter-petal resistances were measured with 18, 19C, 20, 21, 22 and 23 sampled from each petal to which the fixed one doesn't belong. The letter 'C' in the indexes means the copper strand, and 25 and 26C are sampled

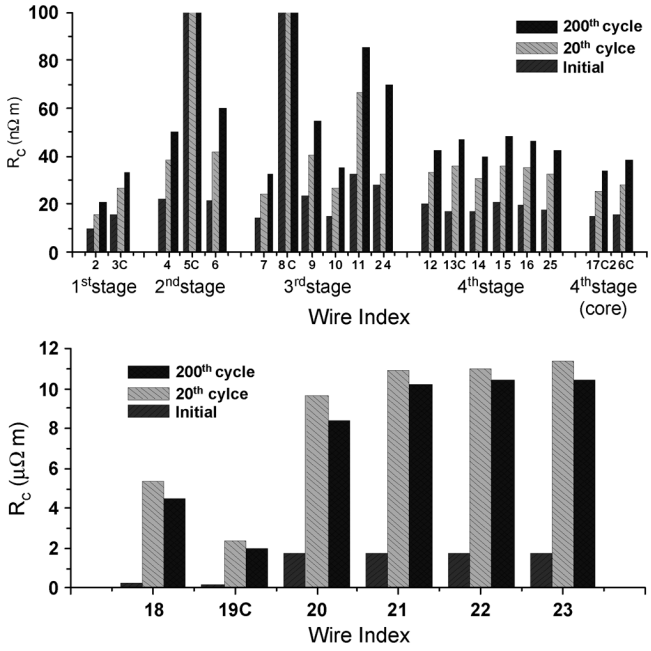

Fig. 4. Measured contact resistance versus wire index of selected strands inside of petal at initial state, after 20th cycle and after 200th cycle (upper) and inter-petal resistances (lower). In this view graphs, all measurements were done without transversal load.

TABLE II
SUMMARY OF AVERAGED RC

Cycles	P (MPa)	Intra-petal R_c (nΩ·m)				Inter-petal R_c (μΩ·m)
		1st stage	2nd stage	3rd stage	4th stage	
1	0	10.29	21.66	22.29	19.38	2.952
	16	10.02	22.00	22.68	19.12	1.462
10	0	13.53	31.19	31.26	27.60	9.407
	16	12.91	30.37	30.40	26.65	1.631
20	0	15.98	40.01	38.05	33.43	9.663
	16	15.55	36.62	34.22	30.98	1.512
100	0	20.65	41.23	44.58	42.78	8.634
	16	18.79	47.19	48.51	38.97	1.138
200	0	21.15	55.02	55.67	43.98	8.766
	16	18.41	47.32	48.30	38.94	0.994

for spares. To put together the result of intra-petal contact resistances with respect to the cabling stage and inter-petal ones as well, measured resistance values were assorted as in Fig. 4, and taken to be averaged by part. Therefore, an overview of contact resistances could be given as shown as in Table II.

At about 100 cycles, the inter-strand resistance of the 1st triplet was being saturated to be stable against repetitive loads, as well as the inter-petal resistance. However, other intra-petal resistances of higher stage tended to be increasing slowly until the maximum number of cycles which we carried out.

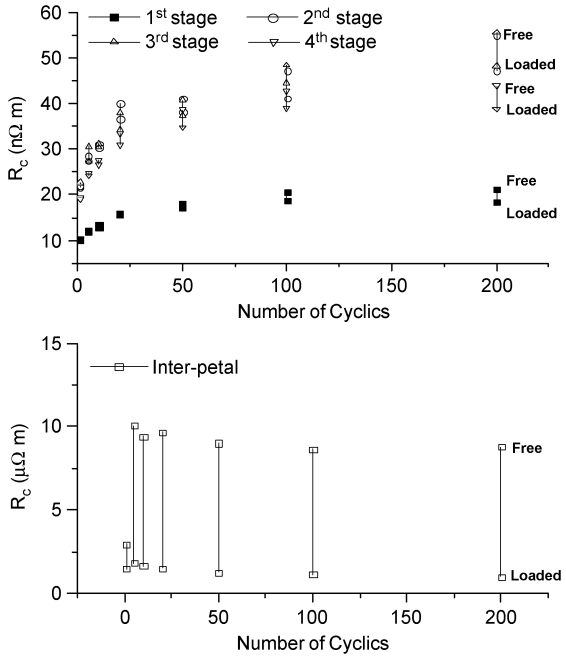

Fig. 5. Evolution of R_cs according to the progress of cyclic loads for intra-petal strands (upper) and inter-petal strands.

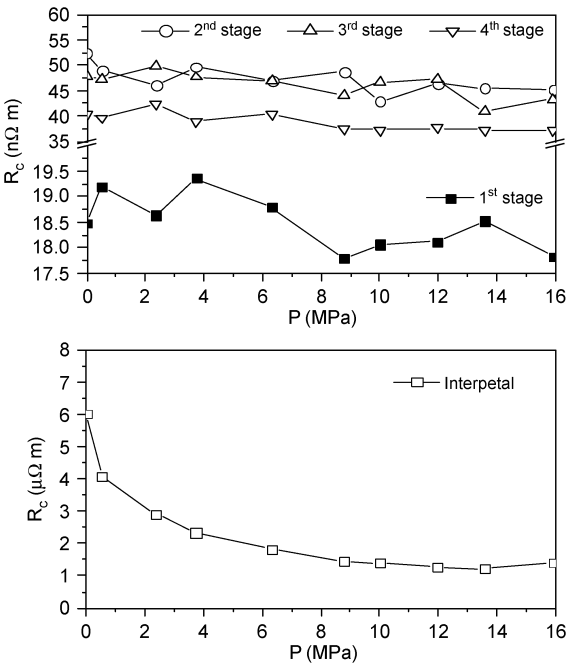

Fig. 6. Pressure dependent contact resistances measured after 100th cycle.

After a few initial cycles with a rapid increase, the inter-petal resistance slowly decreased with respect to the progress of cyclic loads, different from the evolution of intra-petal R_c. A similar dependence of inter-petal resistances already has been reported in the transverse load effect on the ITER TF DP4 conductor [10], but, in our case, the magnitude of evolutions was relatively small.

After 100th cycle, the pressure dependence of contact resistances was recorded as presented as in the Fig. 6. For the intra-petal combinations of strands, only small amount of changes was appeared, on the other hand a quite large decrease of inter-petal resistance was observed, whose factor of magnitude is comparable to the previous reports [5], [10], [11].

IV. Summary and Conclusion

The "Option2" ITER TF conductor was investigated under the repetitive transversal loads employing a specially built device called as VOFEX. Mechanical parameters were obtained from the compressive displacements versus the transversal pressure simulating Lorentz force. Inter-strand resistances were measured with carefully selected strands covering possible combinations of wires between all neighboring stages of cabling for the fixed one. Small variation of contact resistances against the cycles is consistent with the conductor performance of "Option2" samples which was reported in elsewhere [8]. Relatively stable intra-strand resistance was observed under the pressure, which was measured after 100 cycles as well. Even though a tentative stabilization was shown after 100 cycles for inter-petal resistance and inter-strand resistance in 1st triplet, 200 cycles weren't sufficient to make the contact resistance fully stabilized for all components.

References

[1] P. Bruzzone, B. Stepanov, and R. Wesche, "Qualification of ITER TF conductors in SULTAN," *Fusion Engineering and Design*, vol. 94, no. 2/6, pp. 205–209, 2009.

[2] P. Bruzzone, B. Stepanov, R. Wesche, A. Vostner, K. Okuno, I. Isono, Y. Takahashi, H. C. Kim, and K. Kim, "Result of new generation of ITER TF conductor sample in SULTAN," *IEEE Trans. Appl. Supercond.*, vol. 18, pp. 459–462, 2008.

[3] P. Bruzzone, B. Stepanov, M. Bagnasco, M. Calvi, F. Cau, D. Ciazynski, A. d. Corte, A. Di Zenobio, L. Muzzi, A. Nijhuis, and E. Salpietro, "Test results of two European ITER **TF** conductor samples in SULTAN," *IEEE Trans. Appl. Supercond.*, vol. 18, pp. 1188–1091, 2008.

[4] A. Nijhuis and Y. Ilyin, "Transverse load optimization in Nb_3Sn CICC design; influence of cabling, void fraction and strand stiffness," *Superconducting Sci. Tech.*, vol. 19, pp. 945–62, 2006.

[5] A. Nijhuis, N. H. W. Noordman, O. A. Shevchenko, H. H. J. ten Kate, and N. Mitchell, "Electromagnetic and mechanical characterisation of ITER CS-MC conductors affected by transverse cyclic loading: Part2," *IEEE Trans. Appl. Supercond.*, vol. 9, p. 754, 1999.

[6] A. Nijhuis, N. H. W. Noordman, O. A. Shevchenko, H. H. J. ten Kate, and N. Mitchell, "Electromagnetic and mechanical characterisation of ITER CS-MC conductors affected by transverse cyclic loading: Part3," *IEEE Trans. Appl. Supercond.*, vol. 9, p. 165, 1999.

[7] A. Nijhui and Y. Ilylin, "Transverse cable stiffness and mechanical losses associated with load cycles in ITRER Nb_3Sn and NbTi CICC," *Superconducting Sci. Tech.*, vol. 22, p. 055007, 2009.

[8] D. K. Oh, "Performance test of TFKO2 qualification sample of ITER TF conductor," in *Proceedings on the 21th International Conference on Magnet Technology*, Hefei, China, Oct. 21, 2009, to be published.

[9] P. Bruzzone, N. Mitchell, and J. Kuebler, "Mechanical behaviour under transversal load of the 40 kA Nb3Sn cable-in-conduit conductor for the NET inner poloidal coils," in *Proceedings of the 11th International Conference on Magnet Technology*, Tsukuba, Japan, 1989, pp. 926–931.

[10] A. Nijhuis, N. H. W. Noordman, and H. H. J. ten Kate, "Performance of ITER TF DP4 conductor under alternating transverse load in the UT cryogenic press," 1st Intermediate Report of Task 6 for the Contract: NET-98/479 (No.: UT-NET 99-7) Nov. 26, 1999.

[11] A. Nijhuis, N. H. W. Noordman, and H. H. J. ten Kate, "Effect of transverse cyclic loading on the mechanical and electromagnetic behaviour of two ITER CSMC conductors in a cryogenic press," Final Report, Part 1 for the Contract: NET-95/389 (No.: UT-NET 99-1) Oct. 27, 1999.